Published in final edited form as:
ACS Catal. 2021 September 03; 11(17): 10923–10932. doi:10.1021/acscatal.1c02084.

Electric Fields in Catalysis: From Enzymes to Molecular Catalysts

Nadia G. Léonard[§],
Department of Chemistry, University of California, Irvine, California 92697, United States

Rakia Dhaoui[§],
Department of Chemistry, University of California, Irvine, California 92697, United States

Teera Chantarojsiri,
Department of Chemistry and Center of Excellence for Innovation in Chemistry, Faculty of Science, Mahidol University, Bangkok 10400, Thailand

Jenny Y. Yang
Department of Chemistry, University of California, Irvine, California 92697, United States

Abstract

Electric fields underlie all reactions and impact reactivity by interacting with the dipoles and net charges of transition states, products, and reactants to modify the free energy landscape. However, they are rarely given deliberate consideration in synthetic design to rationally control reactivity. This Perspective discusses the commonalities of electric field effects across multiple platforms, from enzymes to molecular catalysts, and identifies practical challenges to applying them in synthetic molecular systems to mediate reactivity.

Graphical Abstract

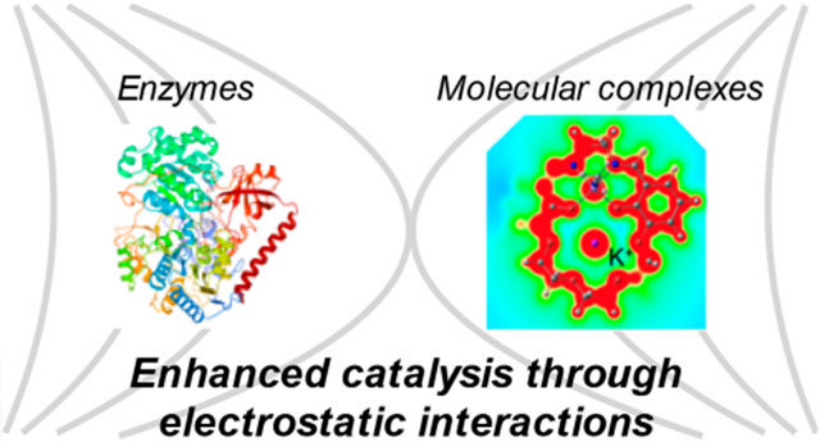

Corresponding Author Jenny Y. Yang – Department of Chemistry, University of California, Irvine, California 92697, United States; j.yang@uci.edu.

[§]Author Contributions
(N.G.L., R.D.) These authors contributed equally.

The authors declare no competing financial interest.

Keywords

electric fields; electrostatics; catalysis; bioinorganic; dipoles; redox reactions; transition metals

Electric fields are believed to be key factors in the superior reactivity and selectivity of enzymatic active sites[1-8] and some zeolites.[9-11] More broadly, electrostatic interactions have been used to rationalize wide ranging reactivity—from enzymatic preorganization and ion-pairing in organocatalysis, to rate enhancement or selectivity control at transition metal complexes. Electric fields in this context stem from either positioned charges, dipoles, or induced dipoles. Modeling these types of interactions are not new. However, renewed interest in using electric fields as "smart reagents" in chemistry[12] highlights the few experimental examples where electric fields are deliberately used as a tool to control reactivity. Electrostatic catalysis places a reacting molecule in an environment that stabilizes the transition state's dipole moment or net charge.[3]

The electric field is defined as the interaction experienced at a given point in space due to the summation of charges, dipoles, and induced dipoles of all other atoms in the system. In most frameworks for modeling, the electric fields experienced by a molecule encompasses the intermolecular field created by other atoms or molecules, but the field created by its own atoms is excluded. Electrostatic interactions are defined as interactions between molecules due to their permanent charges and dipoles.[3] Intrinsic electric fields (such as those in enzymes and zeolites) or applied electric fields (such as those at surfaces, using external applied fields, or STM tips) can be described similarly, with the magnitude of the field dependent on where the field is sampled.[13]

An oriented electrostatic field of appropriate magnitude can direct chemical interactions, reactivity, and catalysis by manipulating activation energies as a function of molecular orientation. Quantum mechanical studies indicate electric fields between 1 and 10 V/nm can adjust activation barriers in the gas phase by several kcal/mol, modifying reaction rates by several orders of magnitude at room temperature.[13] The electric field alters the energy landscape by (1) stabilizing/destabilizing intermediates/transition states which can result in accelerating or prohibiting a reaction pathway and (2) tuning thermodynamic parameters (redox potential, pK_a, bond energy, ground state stabilization or destabilization, etc.). Judicious orientation of an electric field in relation to reacting partners can result in rate enhancement/inhibition,[14-17] changes in mechanism,[18-20] and improved regio- or stereo-selectivity.[21,22] Figure 1 illustrates an example of rate acceleration through stabilization of a transition state by comparing the relative free energies for a reaction in the absence (black trace) and presence (blue trace) of an electric field. For a reaction with a dipolar transition state and a nonpolar reactant, application of an oriented electrostatic field lowers the free energy of the transition state and product relative to the reactants.

Computational modeling and theoretical investigations have been used to understand the principles governing electric field effects on catalysis.[13,23-25] These computational studies, as well as experimental examples, have been discussed in a recently published book[26] and reviews.[5,13,25,27,28] Most experimental studies of controlled electric fields on reactivity have focused on using applied biases[29] such as charged surfaces[30,31] or STM tips[32-35] to generate

fields with magnitudes ranging from 3 to 50 V/nm.[13,27,28] These elegant studies quantify the impact electric fields can have on reaction energies and product selectivity. However, the scalability of these techniques is limited; the reactivity enabled through applied biases is confined to single molecules or electrode surfaces. The magnitude of the electric field also diminishes rapidly with the distance from the external source because of ion and/or solvent screening. Applied biases are also susceptible to dielectric breakdown at high magnitudes, resulting in electron transfer. Additionally, the orientation of the reacting components in relation to the direction of the electric field must be precisely controlled, even when adsorbed on a surface. Exact control of field orientation and magnitude with respect to the reactants is a general challenge with external fields. These factors complicate drawing direct parallels to enzymatic systems or use as a large-scale synthetic tool. Because of these challenges, molecular systems may provide an opportunity to control field orientation with respect to reacting partners due to binding at the reactive center prior to catalysis.

The goal of this Perspective is to highlight specific examples of electric field effects in enzymes, organic reactions, and transition-metal-catalyzed systems. By using select examples and drawing common themes between different catalytic platforms, we aim to show how these commonalities can be used to design platforms with specific electrostatic interactions to achieve reaction control.

ELECTRIC FIELD EFFECTS IN ENZYMES

The efficiency of enzymatic catalysis has long served as a source of inspiration for synthetic chemists. Elucidating the different factors that govern the catalytic power of enzymes is a key step in designing synthetic catalysts that rival the activity of enzymes, from selective C–H activation[36] to energy-efficient CO_2 reduction.[37,38] The overall protein architecture forms microenvironments which exploit a variety of electrostatic interactions and preorganization to aid in catalysis.[1-8] These interactions include hydrogen-bonding networks, proximal Lewis acidic metals or charged functionalities, and the hydrophobicity or hydrophilicity of local active site residues.[39-44]

Warshel pioneered the term electrostatic preorganization as a way to describe the enzymatic environment that favors the transition state rather than the reactants, thus lowering the free energy barrier.[44] Experimental evidence for this electrostatic environment in an enzyme was confirmed by Boxer using vibrational Stark spectroscopy[45] on ketosteroid isomerase (KSI).[46] Specifically, an inhibitor containing a vibrational probe (carbonyl group) was placed in the active site. KSI strongly activates the C═O stretch, where the carbonyl stretching frequency is used as a probe for the electric field. The electric field induced by the protein scaffold on the active site was then found to linearly correlate with the activation free energy of the reaction, providing direct experimental evidence for electrostatic rate enhancement.[47]

In a computational example on the enzyme histone deacetylase 8 (HDAC8), evidence to support the underlying importance of electrostatic preorganization was investigated through the electron charge density.[48] Zinc-dependent HDAC8 catalyzes the deacetylation of a histone lysine and plays a vital role in post-translational modification during the biosynthesis

of proteins.[49] Deacetylation proceeds through formation of an oxyanion intermediate bound to zinc (Figure 2A).[15,40,50] Crystallographic studies of the HDAC8 active site also revealed a K^+ ion buried into the interior of the protein (Figure 2B), approximately 7 Å from the zinc; however, the role of potassium is not understood.[51,52] Computational studies of the zinc-dependent HDAC8 suggest that K^+ plays a role in increasing substrate binding at the central zinc ion and that absence of the K^+ ion causes deactivation of the enzyme. Therefore, the distal K^+ may serve to enhance the electrostatic preorganization at the active site.

In addition to nonredox active metal cations, the electrostatic environment at active sites can also be modulated by charged residues. The active site of chorismite mutase, a metabolic enzyme that catalyzes the rearrangement of chorismite to prephenate, includes a cationic arginine. Replacement of the arginine with neutral citrulline maintains the precise substrate orientation and geometry of the wildtype enzyme but incurs a penalty in catalytic activity.[53] Another example is the formate dehydrogenase (FDH) enzyme. The active site of all known FDHs contain an arginine residue in the secondary coordination sphere.[54] This arginine has been proposed to interact with the negatively charged formate substrate to facilitate C–H bond cleavage.[55]

These three examples serve to highlight the multidimensional roles that electrostatic interactions serve in enzymes. However, there is significant difficulty in strategically pinpointing which individual effects are essential to enzymatic activity, and would thus be critical to emulate within synthetic systems.

ELECTROSTATIC VERSUS LEWIS ACIDITY EFFECTS

While charged metal ions such as alkali and alkaline earth metals leave an electrostatic footprint, they can also serve as Lewis acids. The difference is that in the former case, they are modifying the energy landscape through a noncovalent interaction, and in the latter with a through-bond orbital-overlap interaction. Cation replacement studies are useful for evaluating the relevant electrostatic versus Lewis acidic contributions. For example, the oxygen-evolving complex (OEC) of the photosystem II enzyme (PSII) features a Mn_4CaO_5 core in the active site.[56] Studies aimed at understanding the role of the Ca^{2+} ion in PSII found that displacement with all dicationic alkaline earth metals led to significantly diminished activity with the exception of Sr^{2+}, which has similar Lewis acidity to the Ca^{2+} ion.[57] These studies indicate the Ca^{2+} ion primarily functions as a Lewis acid; if it were mostly providing an electrostatic effect, replacement with any dication would result in similar activity. However, it is worth noting that in cation replacement studies, different ionic radii of alkali and alkaline earth metals may also result in electrostatic perturbations based on changes in distance or geometry to the active site.

Likewise, synthetic catalytic systems often exhibit accelerated rates with Lewis acidic metal cation additives or cocatalysts.[58-67] The Lewis acidic and electrostatic contributions can be decoupled by comparing the relative activity with other additives that are either charged or Lewis acidic, but not both. For example, additives such as noncationic borates can be used to isolate the effect of Lewis acidity. Additionally, quaternary ammonium salts (such

as tetraethylammonium) can be used to introduce a local cationic charge that lacks Lewis acidity.[63,64]

SYNTHETIC SYSTEMS

Various synthetic constructs have been used to generate oriented fields of specific magnitudes across homogeneous active sites. These synthetic systems have the potential to mimic the electrostatic character found in enzymatic active sites.

For example, supramolecular hosts can mimic electrostatic aspects of enzymatic active site cavities (Figure 3A). Multiple parameters, including overall charge, cavity size, and the degree of solvent exclusion can be controlled through synthetic design.[68,69] Prominent examples of charged supramolecular hosts and catalysts that invoke electrostatic effects for their reactivity include Ward and co-workers' $Co_8L_{12}^{16+}$ cube,[70] and Fujita and co-workers' $Pd_6L_4^{12+}$ octahedron.[71] Electrostatic effects in a variety of supramolecular complexes have been examined experimentally[72,73] and with computational studies.[74,75]

Electrostatic interactions have been used extensively to elicit reactivity control in organocatalysis.[76-82] For reactions with proposed transition state structures that are more dipolar than their starting materials or products, it rationally follows that use of electrostatic stabilization would enhance catalysis. Electrostatic interactions have been employed in asymmetric catalysis[83-91] and for site-selective catalysis.[92,93]

Ion pair formation (Figure 3B, the interaction of positively and negatively charged species) occurs to lower the Gibbs free energy (as opposed to ion solvation). Promoting ion-pairing interactions requires that ion–solvent interactions are minimized. In fact, use of highly polar solvents can incur a large energetic penalty to ion-pairing due to solvent reorganization. To minimize this energetic penalty, solvents of relatively low dielectric constant are often used, which can present solubility challenges when cationic/anionic charges are used to generate the electric field. In the early 1990s, Wilcox and co-workers demonstrated the electrostatic acceleration of chemical reactions in nonpolar solvents using intramolecular salt effects.[94-98] Ion-pairing in transition metal complexes[99] has been used to achieve regioselectivity either through directed substrate–ligand interactions,[100-102] steric adjustment,[103] or energetic differentiation of transition states.[104-106] Cation-π interactions have also been utilized to increase the acidity of select C–H bonds; however, this is more of an inductive effect, allowing for site-selective bond activation.[107,108]

Transition metal complexes that incorporate crown ethers to bind cations or have ammonium or sulfonate functionalities in the ligand have emerged as a powerful strategy for accessing tunable electrostatic interactions. These platforms have the potential to provide a predictable, directional, and consistent electric field at each reactive site (Figure 3C,D). However, as discussed below, the accessible magnitudes may be limited depending on solvation.

Most efforts toward ligand-based cation encapsulation in transition metal complexes have focused on applications toward phase transfer and ion sensing[109] or switchable catalysis.[110] There are fewer studies specifically investigating cation encapsulation for electrostatic effects. In order for a cation to impart an electric field at a local reaction site, the cation

must be located in close proximity.[111-119] Otherwise, solvent or other ions in solution will reorient to mitigate the field. Further, solvent reorganization must be minimized in order for the electric field exerted by the cation to affect any transition state stabilization.

We and others have synthesized transition metal complexes with a macrocyclic N_2O_2 Schiff base ligand and an incorporated crown ether (Figure 4).[120-123] The electric field experienced at the redox active metal site by cation M^{n+} manifests itself through significant shifts in the redox potential of up to 600 mV, which corresponds to static electric fields greater than 1 V/nm at the transition metal.[120,124] The sizable shift in redox potential is notable because the measurements are made in solutions containing ~100 fold excess of electrolyte. The rigid positioning of the cation and molecular architecture results in an electric field that is not significantly quenched by solvation or the presence of ions in high concentrations. The Schiff base ligand also contains two imine bonds (–C═N–), which are convenient reporters of the field using vibrational spectroscopy, as evidenced by the Stark shift observed in the complexes.[120] The changes in reduction potential are largely due to the electrostatic contributions that lower the overall energy of the molecular orbitals, which contrasts with modifying reduction potentials using ligand inductive effects.[123] As a result, the addition of the cation leads to unusual reactivity—from disrupting the redox-dependent activity of an aerobic C–H oxidation reaction,[121] to an inverse free energy relationship for an N–N bond formation reaction (vide infra).[122] These changes in reactivity would not be accessible if the reduction potential were tuned using electron-withdrawing and -donating functionalities. Inductive ligand effects alter the ligand field at the metal, modifying the d-orbital splitting. In contrast, the electrostatic potential from the cations shifts the metal-based orbitals relatively uniformly, resulting in unique redox-based reactivity.[123]

Figure 5 illustrates examples of different synthetic transition metal complexes incorporating electrostatic interactions. Agapie and co-workers reported modifications in reduction potential for Mn_xO_y clusters that incorporate nonredox active Lewis acidic heterometal cations. In these systems, the changes in reduction potential correlate with both charge and heterometal Lewis acidity, indicating both electrostatic and inductive effects are involved.[125,126]

Flexible crown-encapsulated cations can influence or tune reactivity, even if they impart a smaller electrostatic effect at the metal. Gilbertson and co-workers found that an iron pyridinediimine complex with a tethered Na^+-encapsulated-crown led to accelerated reduction of nitrite to nitric oxide.[127] In this complex, the cation does not significantly shift the ligand-based reduction potential of the iron complex; instead of directly impacting the iron center, the cation preferentially engages in an electrostatic interaction with the substrate, NO_2^-, for reduction to NO.

Installation of charged functionalities is another synthetic modification to introduce electric fields at active sites. For example, ammonium functionalities on the periphery of iron porphyrin complexes results in accelerated electrocatalytic CO_2 reduction activity due to electrostatic stabilization of a carboxylate intermediate.[128] Proximal ammonium functionalities have also been used to accelerate electrocatalytic oxygen reduction in cobalt and iron porphyrins. For the former, computational studies indicate the cationic

functionalities stabilize anionic intermediates.[129] In the latter example, the proximal cations play a complex role in pre-equilibria substrate binding due to through-space electrostatic and inductive contributions.[130,131] Additionally, Groves and co-workers reported Fe porphyrin complexes with cationic porphyrins that were exceptionally active for C–H activation.[132,133] A subsequent computational study by Shaik and co-workers indicated that the electric field generated by the cationic functionalities selectively destabilized the reactants more than the transition states, leading to the accelerated rate.[134]

Ligand-based electrostatic effects are also expected to impact thermodynamic properties related to hydrogen atom transfer reactions. Tolman and co-workers have explored the effect of cationic (ammonium) and anionic (sulfonate) ligand functionalities on copper hydroxide species. Although the charged functionalities impact the reduction potentials and pK_a, the bond dissociation energies remained relatively constant. However, the kinetic reactivity toward hydrogen atom transfer varies, with cation pairing to the sulfonate functionality, complicating direct attribution to electrostatic effects.[135]

McCrory and co-workers recently demonstrated the use of an *N*-methylpyridinium functionality on a cobalt pyridyldiimine complex to tune the reduction potential of CO_2 reduction catalysis.[136] Incorporation of the charged pyridinium group resulted in higher catalyst activity and a lower overpotential. In another example, Wiedner and co-workers demonstrated enhanced rates and selectivity for MeOH production from CO_2 using a Ru(triphos) hydrogenation catalyst that incorporates a cationic tetraalkylammonium in the ligand backbone.[137] In this example, it is unclear whether the cationic group imparts an inducive effect on the electronic structure of the proposed intermediate dihydrogen complex, lowering its energy, or whether there is through-space stabilization from an internal electric field. The above examples all use cationic functionalities to mediate reactivity by selectively stabilizing reactants or intermediates. However, anionic trifluoroborate groups used in Ni complexes by Anderson and co-workers have also demonstrated accelerated C–F oxidation activity.[138]

Other studies have investigated how electrostatic effects specifically impact the electronic structure of transition metal compounds.[139] Tomson and co-workers investigated a series of tetradentate tris(phosphinimine) Cu(I) complexes that incorporated cationic charges within the secondary coordination sphere.[140] The electrostatic field from the cationic charges results in a modified d-orbital manifold at the metal and significant changes to the Cu(II/I) reduction potential.

Electrostatic effects can also inhibit undesired reaction pathways, such as catalyst deactivation. Catalyst deactivation by bimolecular processes or formation of clusters is a common phenomenon in various catalytic systems.[141] To counter these unproductive pathways, catalysts often use increased steric bulk or site-isolation techniques.[141] However, electrostatic effects can be used to prevent dimerization or oligomerization without the necessity of any support material. Manganese(VI) nitrido complexes supported by Schiff base ligands can bimolecularly couple upon oxidation to generate N_2.[142] Incorporation of cationic charges into the salen framework results in anodic shifts in the Mn(VI/V) reduction potential. Despite an increase in oxidation potential, the rate of bimolecular N–N

bond formation slowed with increasing charge, resulting in an inverse linear free energy relationship.[122] These results illustrate the significant effect charge can play in inhibiting bimolecular reactivity.

OUTLOOK AND CONCLUSIONS

Harnessing the catalytic power of enzymes has enormous potential in developing more robust and efficient synthetic catalysts. As reaction chemists have not yet been able to replicate enzymatic activity or specificity for most reactions, a better understanding for controlling the electric field in reaction microenvironments is necessary. We discuss various synthetic strategies for using oriented electrostatic fields at scalable, homogeneous reaction sites. Microenvironments can be emulated through the construction of supramolecular pores. Precise substrate positioning can be achieved through ion-pair interactions. Local, directional electric fields can be generated through incorporation of cationic metals or charged functional groups. Direct application of these noncovalent interactions and their impact on reactivity and molecular properties will inturn lead to better quantitative descriptions of each approach. We hope that a more deliberate approach toward using electric fields will lead to a more comprehensive understanding of how they facilitate the formation and cleavage of chemical bonds, as well as electron transfer by manipulating activation barriers and intermediate energies.

ACKNOWLEDGMENTS

The authors would like to thank Jahan Dawlaty (USC) for many helpful discussions and feedback and the reviewers for their detailed and insightful comments. N.G.L. would like to thank the UC Presidential Postdoctoral Program for support. R.D. would like to thank NSF Award #2102589. J.Y.Y. would like to thank NIH grant 1R01GM134047-01. T. C. would like to thank the Thailand Research Fund (grant no. MRG6280152) and Mahidol University (Basic Research Fund: fiscal year 2021). J.Y.Y. also acknowledges support as a Sloan Foundation Fellow, a Canadian Institute for Advanced Research (CIFAR) Azrieli Global Scholar in the Bio-Inspired Solar Energy Program, and a Camille Dreyfus Teacher Scholar.

REFERENCES

(1). Warshel A Electrostatic Origin of the Catalytic Power of Enzymes and the Role of Preorganized Active Sites. J. Biol. Chem 1998, 273 (42), 27035–27038. [PubMed: 9765214]

(2). Schramm VL Enzymatic Transition States and Transition State Analog Design. Annu. Rev. Biochem 1998, 67 (1), 693–720. [PubMed: 9759501]

(3). Fried SD; Boxer SG Electric Fields and Enzyme Catalysis. Annu. Rev. Biochem 2017, 86 (1), 387–415. [PubMed: 28375745]

(4). Warshel A; Sharma PK; Kato M; Xiang Y; Liu H; Olsson MHM Electrostatic Basis for Enzyme Catalysis. Chem. Rev. (Washington, DC, U. S.) 2006, 106 (8), 3210–3235.

(5). Li W-L; Head-Gordon T Catalytic Principles from Natural Enzymes and Translational Design Strategies for Synthetic Catalysts. ACS Cent. Sci 2021, 7 (1), 72–80. [PubMed: 33532570]

(6). Wu Y; Fried SD; Boxer SG A Preorganized Electric Field Leads to Minimal Geometrical Reorientation in the Catalytic Reaction of Ketosteroid Isomerase. J. Am. Chem. Soc 2020, 142, 9993. [PubMed: 32378409]

(7). Hanoian P; Liu CT; Hammes-Schiffer S; Benkovic S Perspectives on Electrostatics and Conformational Motions in Enzyme Catalysis. Acc. Chem. Res 2015, 48 (2), 482–489. [PubMed: 25565178]

(8). Liu CT; Layfield JP; Stewart RJ; French JB; Hanoian P; Asbury JB; Hammes-Schiffer S; Benkovic SJ Probing the Electrostatics of Active Site Microenvironments along the Catalytic Cycle for

Escherichia coli Dihydrofolate Reductase. J. Am. Chem. Soc 2014, 136 (29), 10349–10360. [PubMed: 24977791]

(9). Barrachin B; de Lara EC Determination of the electric field in zeolites NaA, NaCaA and Ca6A. Calculation from the ionic charge distribution and infrared measurements of the induced band of N2. J. Chem. Soc., Faraday Trans. 2 1986, 82 (11), 1953–1966.

(10). Rhodes CJ Electric fields in zeolites: fundamental features and environmental implications‡. Chemical Papers 2016, 70 (1), 4–21.

(11). Blatter F; Sun H; Vasenkov S; Frei H Photocatalyzed oxidation in zeolite cages. Catal Today 1998, 41 (4), 297–309.

(12). Shaik S; Mandal D; Ramanan R. Oriented electric fields as future smart reagents in chemistry. Nat. Chem 2016, 8 (12), 1091–1098. [PubMed: 27874869]

(13). Shaik S; Ramanan R; Danovich D; Mandal D Structure and reactivity/selectivity control by oriented-external electric fields. Chem. Soc. Rev 2018, 47 (14), 5125–5145. [PubMed: 29979456]

(14). Meir R; Chen H; Lai W; Shaik S Oriented Electric Fields Accelerate Diels–Alder Reactions and Control the endo/exo Selectivity. ChemPhysChem 2010, 11 (1), 301–310. [PubMed: 19998402]

(15). Schyman P; Lai W; Chen H; Wang Y; Shaik S The Directive of the Protein: How Does Cytochrome P450 Select the Mechanism of Dopamine Formation? J. Am. Chem. Soc 2011, 133 (20), 7977–7984. [PubMed: 21539368]

(16). Shaik S; Shurki A Valence Bond Diagrams and Chemical Reactivity. Angew. Chem., Int. Ed 1999, 38 (5), 586–625.

(17). Shaik S; de Visser SP; Kumar D External Electric Field Will Control the Selectivity of Enzymatic-Like Bond Activations. J. Am. Chem. Soc 2004, 126 (37), 11746–11749. [PubMed: 15366922]

(18). Joy J; Stuyver T; Shaik S Oriented External Electric Fields and Ionic Additives Elicit Catalysis and Mechanistic Cross-over in Oxidative Addition Reactions. J. Am. Chem. Soc 2020, 142, 3836. [PubMed: 31994390]

(19). Stuyver T; Danovich D; De Proft F; Shaik S Electrophilic Aromatic Substitution Reactions: Mechanistic Landscape, Electrostatic and Electric-Field Control of Reaction Rates, and Mechanistic Crossovers. J. Am. Chem. Soc 2019, 141 (24), 9719–9730. [PubMed: 31140274]

(20). Yu L-J; Coote ML Electrostatic Switching between SN1 and SN2 Pathways. J. Phys. Chem. A 2019, 123 (2), 582–589. [PubMed: 30566349]

(21). Zhang M; Zhang F; Xu H; Su Z The regulation of hydroboration of olefins by oriented external electric field. New J. Chem 2018, 42 (22), 18402–18408.

(22). Mattioli EJ; Bottoni A; Zerbetto F; Calvaresi M Oriented External Electric Fields Affect Rate and Stereoselectivity of Electrocyclic Reactions. J. Phys. Chem. C 2019, 123 (43), 26370–26378.

(23). Stuyver T; Danovich D; Joy J; Shaik S External electric field effects on chemical structure and reactivity. Wiley Interdiscip. Rev.: Comput. Mol. Sci 2020, 10 (2), e1438.

(24). Welborn VV; Pestana LR; Head-Gordon T Computational optimization of electric fields for better catalysis design. Nature Catalysis 2018, 1 (9), 649–655.

(25). Shaik S; Danovich D; Joy J; Wang Z; Stuyver T Electric-field mediated chemistry: uncovering and exploiting the potential of (oriented) electric fields to exert chemical catalysis and reaction control. J. Am. Chem. Soc 2020, 142, 12551. [PubMed: 32551571]

(26). Shaik S; Stuyver T Effects of Electric Fields on Structure and Reactivity: New Horizons in Chemistry; Royal Society of Chemistry: 2021.

(27). Ciampi S; Darwish N; Aitken HM; Díez-Pérez I; Coote ML Harnessing electrostatic catalysis in single molecule, electrochemical and chemical systems: a rapidly growing experimental tool box. Chem. Soc. Rev 2018, 47 (14), 5146–5164. [PubMed: 29947390]

(28). Che F; Gray JT; Ha S; Kruse N; Scott SL; McEwen J-S Elucidating the Roles of Electric Fields in Catalysis: A Perspective. ACS Catal. 2018, 8 (6), 5153–5174.

(29). Vogel YB; Zhang L; Darwish N; Gonçales VR; Le Brun A; Gooding JJ; Molina A; Wallace GG; Coote ML; Gonzalez J; Ciampi S Reproducible flaws unveil electrostatic aspects of semiconductor electrochemistry. Nat. Commun 2017, 8 (1), 2066. [PubMed: 29233986]

(30). Gorin CF; Beh ES; Kanan MW An Electric Field–Induced Change in the Selectivity of a Metal Oxide–Catalyzed Epoxide Rearrangement. J. Am. Chem. Soc 2012, 134 (1), 186–189. [PubMed: 22191979]

(31). Gorin CF; Beh ES; Bui QM; Dick GR; Kanan MW Interfacial Electric Field Effects on a Carbene Reaction Catalyzed by Rh Porphyrins. J. Am. Chem. Soc 2013, 135 (30), 11257–11265. [PubMed: 23837635]

(32). Aragonès AC; Haworth NL; Darwish N; Ciampi S; Bloomfield NJ; Wallace GG; Diez-Perez I; Coote ML Electrostatic catalysis of a Diels–Alder reaction. Nature 2016, 531 (7592), 88–91. [PubMed: 26935697]

(33). Zhang L; Laborda E; Darwish N; Noble BB; Tyrell JH; Pluczyk S; Le Brun AP; Wallace GG; Gonzalez J; Coote ML; Ciampi S Electrochemical and Electrostatic Cleavage of Alkoxyamines. J. Am. Chem. Soc 2018, 140 (2), 766–774. [PubMed: 29258306]

(34). Huang X; Tang C; Li J; Chen L-C; Zheng J; Zhang P; Le J; Li R; Li X; Liu J; Yang Y; Shi J; Chen Z; Bai M; Zhang H-L; Xia H; Cheng J; Tian Z-Q; Hong W Electric field–induced selective catalysis of single-molecule reaction. Science Advances 2019, 5 (6), eaaw3072. [PubMed: 31245539]

(35). Alemani M; Peters MV; Hecht S; Rieder K-H; Moresco F; Grill L Electric Field-Induced Isomerization of Azobenzene by STM. J. Am. Chem. Soc 2006, 128 (45), 14446–14447. [PubMed: 17090013]

(36). Wang VC-C; Maji S; Chen PP-Y; Lee HK; Yu SS-F; Chan SI Alkane Oxidation: Methane Monooxygenases, Related Enzymes, and Their Biomimetics. Chem. Rev 2017, 117, 8574–8621. [PubMed: 28206744]

(37). Bassegoda A; Madden C; Wakerley DW; Reisner E; Hirst J Reversible Interconversion of CO2 and Formate by a Molybdenum-Containing Formate Dehydrogenase. J. Am. Chem. Soc 2014, 136 (44), 15473–15476. [PubMed: 25325406]

(38). Parkin A; Seravalli J; Vincent KA; Ragsdale SW; Armstrong FA Rapid and Efficient Electrocatalytic CO2/CO Interconversions by Carboxydothermus hydrogenoformans CO Dehydrogenase I on an Electrode. J. Am. Chem. Soc 2007, 129 (34), 10328–10329. [PubMed: 17672466]

(39). Nechay MR; Gallup NM; Morgenstern A; Smith QA; Eberhart ME; Alexandrova AN Histone Deacetylase 8:Characterization of Physiological Divalent Metal Catalysis. J. Phys. Chem. B 2016, 120 (26), 5884–5895. [PubMed: 26996235]

(40). Corminboeuf C; Hu P; Tuckerman ME; Zhang Y Unexpected Deacetylation Mechanism Suggested by a Density Functional Theory QM/MM Study of Histone-Deacetylase-Like Protein. J. Am. Chem. Soc 2006, 128 (14), 4530–4531. [PubMed: 16594663]

(41). Gilson MK; Honig BH Calculation of electrostatic potentials in an enzyme active site. Nature 1987, 330 (6143), 84–86. [PubMed: 3313058]

(42). Sigala PA; Fafarman AT; Bogard PE; Boxer SG; Herschlag D Do Ligand Binding and Solvent Exclusion Alter the Electrostatic Character within the Oxyanion Hole of an Enzymatic Active Site? J. Am. Chem. Soc 2007, 129 (40), 12104–12105. [PubMed: 17854190]

(43). Sun DP; Liao DI; Remington SJ Electrostatic fields in the active sites of lysozymes. Proc. Natl. Acad. Sci. U. S. A 1989, 86 (14), 5361–5365. [PubMed: 2664781]

(44). Warshel A Electrostatic basis of structure-function correlation in proteins. Acc. Chem. Res 1981, 14 (9), 284–290.

(45). Fried SD; Boxer SG Measuring Electric Fields and Noncovalent Interactions Using the Vibrational Stark Effect. Acc. Chem. Res 2015, 48 (4), 998–1006. [PubMed: 25799082]

(46). Fried SD; Bagchi S; Boxer SG Extreme electric fields power catalysis in the active site of ketosteroid isomerase. Science 2014, 346 (6216), 1510–1514. [PubMed: 25525245]

(47). Wu Y; Boxer SG A Critical Test of the Electrostatic Contribution to Catalysis with Noncanonical Amino Acids in Ketosteroid Isomerase. J. Am. Chem. Soc 2016, 138 (36), 11890–11895. [PubMed: 27545569]

(48). Morgenstern A; Jaszai M; Eberhart ME; Alexandrova AN Quantified electrostatic preorganization in enzymes using the geometry of the electron charge density. Chemical Science 2017, 8 (7), 5010–5018. [PubMed: 28970888]

(49). Drazic A; Myklebust LM; Ree R; Arnesen T The world of protein acetylation. Biochim. Biophys. Acta, Proteins Proteomics 2016, 1864 (10), 1372–1401.

(50). Wu R; Wang S; Zhou N; Cao Z; Zhang Y A Proton-Shuttle Reaction Mechanism for Histone Deacetylase 8 and the Catalytic Role of Metal Ions. J. Am. Chem. Soc 2010, 132 (27), 9471–9479. [PubMed: 20568751]

(51). Vannini A; Volpari C; Gallinari P; Jones P; Mattu M; Carfí A; De Francesco R; Steinkühler C; Di Marco S Substrate binding to histone deacetylases as shown by the crystal structure of the HDAC8–substrate complex. EMBO Rep. 2007, 8 (9), 879–884. [PubMed: 17721440]

(52). Somoza JR; Skene RJ; Katz BA; Mol C; Ho JD; Jennings AJ; Luong C; Arvai A; Buggy JJ; Chi E; Tang J; Sang B-C; Verner E; Wynands R; Leahy EM; Dougan DR; Snell G; Navre M; Knuth MW; Swanson RV; McRee DE; Tari LW Structural Snapshots of Human HDAC8 Provide Insights into the Class I Histone Deacetylases. Structure 2004, 12 (7), 1325–1334. [PubMed: 15242608]

(53). Štrajbl M; Shurki A; Kato M; Warshel A Apparent NAC Effect in Chorismate Mutase Reflects Electrostatic Transition State Stabilization. J. Am. Chem. Soc 2003, 125 (34), 10228–10237. [PubMed: 12926945]

(54). Maia LB; Moura I; Moura JJG Molybdenum and tungsten-containing formate dehydrogenases: Aiming to inspire a catalyst for carbon dioxide utilization. Inorg. Chim. Acta 2017, 455, 350–363.

(55). Niks D; Duvvuru J; Escalona M; Hille R Spectroscopic and Kinetic Properties of the Molybdenum-containing, NAD+-dependent Formate Dehydrogenase from Ralstonia eutropha*. J. Biol. Chem 2016, 291 (3), 1162–1174. [PubMed: 26553877]

(56). Umena Y; Kawakami K; Shen J-R; Kamiya N Crystal structure of oxygen-evolving photosystem II at a resolution of 1.9 Å. Nature 2011, 473 (7345), 55–60. [PubMed: 21499260]

(57). Lee C-I; Lakshmi KV; Brudvig GW Probing the Functional Role of Ca2+ in the Oxygen-Evolving Complex of Photosystem II by Metal Ion Inhibition. Biochemistry 2007, 46 (11), 3211–3223. [PubMed: 17309233]

(58). Morimoto Y; Kotani H; Park J; Lee Y-M; Nam W; Fukuzumi S Metal Ion-Coupled Electron Transfer of a Nonheme Oxoiron(IV) Complex: Remarkable Enhancement of Electron-Transfer Rates by Sc3+. J. Am. Chem. Soc 2011, 133 (3), 403–405. [PubMed: 21158434]

(59). Grubel K; Brennessel WW; Mercado BQ; Holland PL Alkali Metal Control over N–N Cleavage in Iron Complexes. J. Am. Chem. Soc 2014, 136 (48), 16807–16816. [PubMed: 25412468]

(60). Bernskoetter WH; Hazari N Reversible Hydrogenation of Carbon Dioxide to Formic Acid and Methanol: Lewis Acid Enhancement of Base Metal Catalysts. Acc. Chem. Res 2017, 50 (4), 1049–1058. [PubMed: 28306247]

(61). Bertini F; Glatz M; Gorgas N; Stöger B; Peruzzini M; Veiros LF; Kirchner K; Gonsalvi L Carbon dioxide hydrogenation catalysed by well-defined Mn(i) PNP pincer hydride complexes. Chemical Science 2017, 8 (7), 5024–5029. [PubMed: 28970889]

(62). Siek S; Burks DB; Gerlach DL; Liang G; Tesh JM; Thompson CR; Qu F; Shankwitz JE; Vasquez RM; Chambers N; Szulczewski GJ; Grotjahn DB; Webster CE; Papish ET Iridium and Ruthenium Complexes of N-Heterocyclic Carbene- and Pyridinol-Derived Chelates as Catalysts for Aqueous Carbon Dioxide Hydrogenation and Formic Acid Dehydrogenation: The Role of the Alkali Metal. Organometallics 2017, 36 (6), 1091–1106. [PubMed: 29540958]

(63). Heimann JE; Bernskoetter WH; Hazari N Understanding the Individual and Combined Effects of Solvent and Lewis Acid on CO2 Insertion into a Metal Hydride. J. Am. Chem. Soc 2019, 141 (26), 10520–10529. [PubMed: 31244180]

(64). Heimann JE; Bernskoetter WH; Hazari N; Mayer JM Acceleration of CO2 insertion into metal hydrides: ligand, Lewis acid, and solvent effects on reaction kinetics. Chemical Science 2018, 9 (32), 6629–6638. [PubMed: 30310595]

(65). Park YJ; Ziller JW; Borovik AS The Effects of Redox-Inactive Metal Ions on the Activation of Dioxygen: Isolation and Characterization of a Heterobimetallic Complex Containing a MnIII–(μ-OH)–CaII Core. J. Am. Chem. Soc 2011, 133 (24), 9258–9261. [PubMed: 21595481]

(66). Miller CG; Gordon-Wylie SW; Horwitz CP; Strazisar SA; Peraino DK; Clark GR; Weintraub ST; Collins TJ A Method for Driving O-Atom Transfer: Secondary Ion Binding to a Tetraamide Macrocyclic Ligand. J. Am. Chem. Soc 1998, 120 (44), 11540–11541.

(67). Zhang J; Sha S-C; Bellomo A; Trongsiriwat N; Gao F; Tomson NC; Walsh PJ Positional Selectivity in C–H Functionalizations of 2-Benzylfurans with Bimetallic Catalysts. J. Am. Chem. Soc 2016, 138 (12), 4260–4266. [PubMed: 26937718]

(68). Hastings CJ; Bergman RG; Raymond KN Origins of Large Rate Enhancements in the Nazarov Cyclization Catalyzed by Supramolecular Encapsulation. Chem. - Eur. J 2014, 20 (14), 3966–3973. [PubMed: 24615703]

(69). Frushicheva MP; Mukherjee S; Warshel A Electrostatic Origin of the Catalytic Effect of a Supramolecular Host Catalyst. J. Phys. Chem. B 2012, 116 (45), 13353–13360. [PubMed: 23088306]

(70). Cullen W; Misuraca MC; Hunter CA; Williams NH; Ward MD Highly efficient catalysis of the Kemp elimination in the cavity of a cubic coordination cage. Nat. Chem 2016, 8 (3), 231–236. [PubMed: 26892554]

(71). Yoshizawa M; Tamura M; Fujita M Diels-Alder in Aqueous Molecular Hosts: Unusual Regioselectivity and Efficient Catalysis. Science 2006, 312 (5771), 251–254. [PubMed: 16614218]

(72). Morimoto M; Bierschenk SM; Xia KT; Bergman RG; Raymond KN; Toste FD Advances in supramolecular host-mediated reactivity. Nature Catalysis 2020, 3 (12), 969–984.

(73). Hong CM; Bergman RG; Raymond KN; Toste FD Self-Assembled Tetrahedral Hosts as Supramolecular Catalysts. Acc. Chem. Res 2018, 51 (10), 2447–2455. [PubMed: 30272943]

(74). Welborn VV; Li W-L; Head-Gordon T Interplay of water and a supramolecular capsule for catalysis of reductive elimination reaction from gold. Nat. Commun 2020, 11 (1), 415. [PubMed: 31964874]

(75). Vaissier Welborn V; Head-Gordon T Electrostatics Generated by a Supramolecular Capsule Stabilizes the Transition State for Carbon–Carbon Reductive Elimination from Gold(III) Complex. J. Phys. Chem. Lett 2018, 9 (14), 3814–3818. [PubMed: 29939756]

(76). Neel AJ; Hilton MJ; Sigman MS; Toste FD Exploiting non-covalent π interactions for catalyst design. Nature 2017, 543 (7647), 637–646. [PubMed: 28358089]

(77). Yamada S Cation–π Interactions in Organic Synthesis. Chem. Rev 2018, 118 (23), 11353–11432. [PubMed: 30507123]

(78). Wheeler SE; Seguin TJ; Guan Y; Doney AC Noncovalent Interactions in Organocatalysis and the Prospect of Computational Catalyst Design. Acc. Chem. Res 2016, 49 (5), 1061–1069. [PubMed: 27110641]

(79). Dhayalan V; Gadekar SC; Alassad Z; Milo A Unravelling mechanistic features of organocatalysis with in situ modifications at the secondary sphere. Nat. Chem 2019, 11 (6), 543–551. [PubMed: 31086303]

(80). Dougherty DA The Cation–π Interaction. Acc. Chem. Res 2013, 46 (4), 885–893. [PubMed: 23214924]

(81). Kennedy CR; Lin S; Jacobsen EN The Cation–π Interaction in Small-Molecule Catalysis. Angew. Chem., Int. Ed 2016, 55 (41), 12596–12624.

(82). Zhao Y; Cotelle Y; Liu L; López-Andarias J; Bornhof A-B; Akamatsu M; Sakai N; Matile S The Emergence of Anion–π Catalysis. Acc. Chem. Res 2018, 51 (9), 2255–2263. [PubMed: 30188692]

(83). Knowles RR; Jacobsen EN Attractive noncovalent interactions in asymmetric catalysis: Links between enzymes and small molecule catalysts. Proc. Natl. Acad. Sci. U. S. A 2010, 107 (48), 20678–20685. [PubMed: 20956302]

(84). Brak K; Jacobsen EN Asymmetric Ion-Pairing Catalysis. Angew. Chem., Int. Ed 2013, 52 (2), 534–561.

(85). DiRocco DA; Noey EL; Houk KN; Rovis T Catalytic Asymmetric Intermolecular Stetter Reactions of Enolizable Aldehydes with Nitrostyrenes: Computational Study Provides Insight into the Success of the Catalyst. Angew. Chem., Int. Ed 2012, 51 (10), 2391–2394.

(86). Lee K; Silverio DL; Torker S; Robbins DW; Haeffner F; van der Mei FW; Hoveyda AH Catalytic enantioselective addition of organoboron reagents to fluoroketones controlled by electrostatic interactions. Nat. Chem 2016, 8 (8), 768–777. [PubMed: 27442282]

(87). Kennedy CR; Guidera JA; Jacobsen EN Synergistic Ion-Binding Catalysis Demonstrated via an Enantioselective, Catalytic [2,3]-Wittig Rearrangement. ACS Cent. Sci 2016, 2 (6), 416–423. [PubMed: 27413786]

(88). Maji R; Wheeler SE Importance of Electrostatic Effects in the Stereoselectivity of NHC-Catalyzed Kinetic Resolutions. J. Am. Chem. Soc 2017, 139 (36), 12441–12449. [PubMed: 28823166]

(89). Seguin TJ; Wheeler SE Electrostatic Basis for Enantioselective Brønsted-Acid-Catalyzed Asymmetric Ring Openings of meso-Epoxides. ACS Catal. 2016, 6 (4), 2681–2688.

(90). Seguin TJ; Wheeler SE Stacking and Electrostatic Interactions Drive the Stereoselectivity of Silylium-Ion Asymmetric Counteranion-Directed Catalysis. Angew. Chem., Int. Ed 2016, 55 (51), 15889–15893.

(91). Doney AC; Rooks BJ; Lu T; Wheeler SE Design of Organocatalysts for Asymmetric Propargylations through Computational Screening. ACS Catal. 2016, 6 (11), 7948–7955.

(92). Xiao G; Cintron-Rosado GA; Glazier DA; Xi B.-m.; Liu C; Liu P; Tang W Catalytic Site-Selective Acylation of Carbohydrates Directed by Cation–n Interaction. J. Am. Chem. Soc 2017, 139 (12), 4346–4349. [PubMed: 28297601]

(93). Toste FD; Sigman MS; Miller SJ Pursuit of Noncovalent Interactions for Strategic Site-Selective Catalysis. Acc. Chem. Res 2017, 50 (3), 609–615. [PubMed: 28945415]

(94). Smith PJ; Wilcox CS The chemistry of synthetic receptors and functional group arrays. 13. The intramolecular salt effect. J. Org. Chem 1990, 55 (22), 5675–5678.

(95). Smith PJ; Wilcox CS The chemistry of functional group arrays. Electrostatic catalysis and the “intramolecular salt effect. Tetrahedron 1991, 47 (14), 2617–2628.

(96). Smith PJ; Kim E.-i.; Wilcox CS Substrate-Specific Catalysis by Ion Pairs. Angew. Chem., Int. Ed. Engl 1993, 32 (11), 1648–1650.

(97). Kim E.-i.; Paliwal S; Wilcox CS Measurements of Molecular Electrostatic Field Effects in Edge-to-Face Aromatic Interactions and CH-π Interactions with Implications for Protein Folding and Molecular Recognition. J. Am. Chem. Soc 1998, 120 (43), 11192–11193.

(98). Raposo C; Wilcox CS The intramolecular salt effect in chiral auxiliaries. Enhanced diastereoselectivity in a nitrile oxide cycloaddition via rational transition state stabilization. Tetrahedron Lett. 1999, 40 (7), 1285–1288.

(99). Davis HJ; Phipps RJ Harnessing non-covalent interactions to exert control over regioselectivity and site-selectivity in catalytic reactions. Chemical Science 2017, 8 (2), 864–877. [PubMed: 28572898]

(100). Chattopadhyay B; Dannatt JE; Andujar-De Sanctis IL; Gore KA; Maleczka RE; Singleton DA; Smith MR Ir-Catalyzed ortho-Borylation of Phenols Directed by Substrate–Ligand Electrostatic Interactions: A Combined Experimental/in Silico Strategy for Optimizing Weak Interactions. J. Am. Chem. Soc 2017, 139 (23), 7864–7871. [PubMed: 28453268]

(101). Yang L; Uemura N; Nakao Y meta-Selective C–H Borylation of Benzamides and Pyridines by an Iridium-Lewis Acid Bifunctional Catalyst. J. Am. Chem. Soc 2019, 141 (19), 7972–7979. [PubMed: 31017408]

(102). Olivo G; Capocasa G; Lanzalunga O; Di Stefano S; Costas M Enzyme-like substrate-selectivity in C–H oxidation enabled by recognition. Chem. Commun 2019, 55 (7), 917–920.

(103). Montero Bastidas JR; Oleskey TJ; Miller SL; Smith MR; Maleczka RE Para-Selective, Iridium-Catalyzed C–H Borylations of Sulfated Phenols, Benzyl Alcohols, and Anilines Directed by Ion-Pair Electrostatic Interactions. J. Am. Chem. Soc 2019, 141 (39), 15483–15487. [PubMed: 31525037]

(104). Lau VM; Pfalzgraff WC; Markland TE; Kanan MW Electrostatic Control of Regioselectivity in Au(I)-Catalyzed Hydro-arylation. J. Am. Chem. Soc 2017, 139 (11), 4035–4041. [PubMed: 28225605]

(105). Lavallo V; Wright JH II; Tham FS; Quinlivan S Perhalogenated Carba-closo-dodecaborate Anions as Ligand Substituents: Applications in Gold Catalysis. Angew. Chem., Int. Ed 2013, 52 (11), 3172–3176.

(106). Chan AL; Estrada J; Kefalidis CE; Lavallo V Changing the Charge: Electrostatic Effects in Pd-Catalyzed Cross-Coupling. Organometallics 2016, 35 (19), 3257–3260.

(107). Sha S-C; Tcyrulnikov S; Li M; Hu B; Fu Y; Kozlowski MC; Walsh PJ Cation–π Interactions in the Benzylic Arylation of Toluenes with Bimetallic Catalysts. J. Am. Chem. Soc 2018, 140 (39), 12415–12423. [PubMed: 30185030]

(108). Batuecas M; Luo J; Gergelitsová I; Krämer K; Whitaker D; Vitorica-Yrezabal IJ; Larrosa I Catalytic Asymmetric C–H Arylation of (η6-Arene)Chromium Complexes: Facile Access to Planar-Chiral Phosphines. ACS Catal. 2019, 9 (6), 5268–5278. [PubMed: 32064145]

(109). van Veggel FCJM; Verboom W; Reinhoudt DN Metallomacrocycles: Supramolecular Chemistry with Hard and Soft Metal Cations in Action. Chem. Rev 1994, 94 (2), 279–299.

(110). Yoo C; Dodge HM; Miller AJM Cation-controlled catalysis with crown ether-containing transition metal complexes. Chem. Commun. (Cambridge, U. K.) 2019, 55 (35), 5047–5059.

(111). Powell J; Kuksis A; May CJ; Nyburg SC; Smith SJ Chelating phosphinite complexes of Group 6 metal carbonyls with crown-ether-type characteristics. Effect of preferential cation binding on the reactivity of coordinated carbon monoxide. J. Am. Chem. Soc 1981, 103 (19), 5941–5943.

(112). Powell J; Gregg M; Kuksis A; Meindl P Phosphorus donor-crown ether hybrid ligands as a route to carbonyl activation: phosphorus substituent effects and the importance of strong cation binding. J. Am. Chem. Soc 1983, 105 (4), 1064–1065.

(113). Van Staveren CJ; Fenton DE; Reinhoudt DN; Van Eerden J; Harkema S Co-complexation of urea and UO22+ in a Schiff base macrocycle: a mimic of an enzyme binding site. J. Am. Chem. Soc 1987, 109 (11), 3456–3458.

(114). van Veggel FCJM; Bos M; Harkema S; Verboom W; Reinhoudt DN The Organization of Two “Soft” (Cu2⊕, Ni2⊕) Metal Centers in Heterotrinuclear Complexes of a Macrocyclic Ligand by Cocomplexation with Ba2⊕. Angew. Chem., Int. Ed. Engl 1989, 28 (6), 746–748.

(115). Van Veggel FCJM; Harkema S; Bos M; Verboom W; Van Staveren CJ; Gerritsma GJ; Reinhoudt DN Metallomacrocycles: synthesis, x-ray structure, electrochemistry, and ESR spectroscopy of mononuclear and heterodinuclear complexes. Inorg. Chem 1989, 28 (6), 1133–1148.

(116). Puntener K; Hellman MD; Kuester E; Hegedus LS Synthesis and Complexation Properties of Poly(ethylene glycol)-Linked Mono- and Bis-dioxocyclams. J. Org. Chem 2000, 65 (24), 8301–8306. [PubMed: 11101389]

(117). Habata Y; Ikeda M; Sah AK; Noto K; Kuwahara S Selective Retention of Methanol over Ethanol by a Cyclen-Based Cryptand/Copper(II) Complex. Inorg. Chem 2013, 52, 11697. [PubMed: 24102248]

(118). Balch AL; Rowley SP Solubilizing the thallium-platinum unit of Tl2Pt(CN)4. Preparation and use of a new crown ether/phosphine hybrid ligand for linking main-group and transition-metal ions. J. Am. Chem. Soc 1990, 112 (16), 6139–6140.

(119). Balch AL; Neve F; Olmstead MM Assessing the effects of metal ion proximity on a trans-Ir(CO)Cl(phosphine)2 unit. Structural studies of potassium(I), Tin(II), and Lead(II) complexes of (crown-P2)Ir(CO)Cl. Inorg. Chem 1991, 30 (18), 3395–3402.

(120). Reath AH; Ziller JW; Tsay C; Ryan AJ; Yang JY Redox Potential and Electronic Structure Effects of Proximal Nonredox Active Cations in Cobalt Schiff Base Complexes. Inorg. Chem 2017, 56 (6), 3713–3718. [PubMed: 28240885]

(121). Chantarojsiri T; Ziller JW; Yang JY Incorporation of redox-inactive cations promotes iron catalyzed aerobic C–H oxidation at mild potentials. Chemical Science 2018, 9 (9), 2567–2574. [PubMed: 29732136]

(122). Chantarojsiri T; Reath AH; Yang JY Cationic Charges Leading to an Inverse Free-Energy Relationship for N–N Bond Formation by MnVI Nitrides. Angew. Chem., Inf. Ed 2018, 57 (43), 14037–14042.

(123). Kang K; Fuller J; Reath AH; Ziller JW; Alexandrova AN; Yang JY Installation of internal electric fields by non-redox active cations in transition metal complexes. Chemical Science 2019, 10 (43), 10135–10142. [PubMed: 32015820]

(124). Kumar A; Lionetti D; Day VW; Blakemore JD Redox-Inactive Metal Cations Modulate the Reduction Potential of the Uranyl Ion in Macrocyclic Complexes. J. Am. Chem. Soc 2020, 142 (6), 3032–3041. [PubMed: 31927996]

(125). Tsui EY; Tran R; Yano J; Agapie T Redox-inactive metals modulate the reduction potential in heterometallic manganese–oxido clusters. Nat. Chem 2013, 5 (4), 293–299. [PubMed: 23511417]

(126). Tsui EY; Agapie T Reduction potentials of heterometallic manganese–oxido cubane complexes modulated by redox-inactive metals. Proc. Natl. Acad. Sci. U. S. A 2013, 110 (25), 10084. [PubMed: 23744039]

(127). Burns KT; Marks WR; Cheung PM; Seda T; Zakharov LN; Gilbertson JD Uncoupled Redox-Inactive Lewis Acids in the Secondary Coordination Sphere Entice Ligand-Based Nitrite Reduction. Inorg. Chem 2018, 57 (16), 9601–9610. [PubMed: 29608297]

(128). Azcarate I; Costentin C; Robert M; Savéant J-M Through-Space Charge Interaction Substituent Effects in Molecular Catalysis Leading to the Design of the Most Efficient Catalyst of CO2-to-CO Electrochemical Conversion. J. Am. Chem. Soc 2016, 138 (51), 16639–16644. [PubMed: 27976580]

(129). Zhang R; Warren JJ Controlling the Oxygen Reduction Selectivity of Asymmetric Cobalt Porphyrins by Using Local Electrostatic Interactions. J. Am. Chem. Soc 2020, 142 (31), 13426–13434. [PubMed: 32706247]

(130). Martin DJ; Mercado BQ; Mayer JM Combining scaling relationships overcomes rate versus overpotential trade-offs in O_2 molecular electrocatalysis. Science Advances 2020, 6 (11), eaaz3318. [PubMed: 32201730]

(131). Martin DJ; Mercado BQ; Mayer JM All Four Atropisomers of Iron Tetra(o-N,N,N-trimethylanilinium)porphyrin in Both the Ferric and Ferrous States. Inorg. Chem 2021, 60 (7), 5240–5251. [PubMed: 33749269]

(132). Gao H; Groves JT Fast Hydrogen Atom Abstraction by a Hydroxo Iron(III) Porphyrazine. J. Am. Chem. Soc 2017, 139 (11), 3938–3941. [PubMed: 28245648]

(133). Bell SR; Groves JT A Highly Reactive P450 Model Compound I. J. Am. Chem. Soc 2009, 131 (28), 9640–9641. [PubMed: 19552441]

(134). Stuyver T; Ramanan R; Mallick D; Shaik S Oriented (Local) Electric Fields Drive the Millionfold Enhancement of the H-Abstraction Catalysis Observed for Synthetic Metalloenzyme Analogues. Angew. Chem., Int. Ed 2020, 59 (20), 7915–7920.

(135). Dhar D; Yee GM; Tolman WB Effects of Charged Ligand Substituents on the Properties of the Formally Copper(III)-Hydroxide ([CuOH]2+) Unit. Inorg. Chem 2018, 57 (16), 9794–9806. [PubMed: 30070473]

(136). Nie W; Tarnopol DE; McCrory CCL Enhancing a Molecular Electrocatalyst's Activity for CO2 Reduction by Simultaneously Modulating Three Substituent Effects. J. Am. Chem. Soc 2021, 143 (10), 3764–3778. [PubMed: 33683865]

(137). Erickson JD; Preston AZ; Linehan JC; Wiedner ES Enhanced Hydrogenation of Carbon Dioxide to Methanol by a Ruthenium Complex with a Charged Outer-Coordination Sphere. ACS Catal. 2020, 10 (13), 7419–7423.

(138). Kelty ML; McNeece AJ; Filatov AS; Anderson J Electrostatic vs. Inductive Effects in Phosphine Ligand Donor Properties, Reactivity, and Catalysis. ChemRxiv. Cambridge: Cambridge Open Engage; 2021; This content is a preprint and has not been peer-reviewed.

(139). Few experimental studies have explicitly investigated the effects of electrostatics on transition metal electronic structure. Salient computational studies are included here. (a) Shaik S; de Visser SP; Kumar D External Electric Field Will Control the Selectivity of Enzymatic-Like Bond Activations. J. Am. Chem. Soc 2004, 126 (37), 11746–11749 [PubMed: 15366922] (b)Joy J; Stuyver T; Shaik S Oriented External Electric Fields and Ionic Additives Elicit Catalysis and Mechanistic Cross-over in Oxidative Addition Reactions. J. Am. Chem. Soc 2020, 142, 3836. [PubMed: 31994390]

(140). Weberg AB; McCollom SP; Thierer LM; Gau MR; Carroll PJ; Tomson NC Using internal electrostatic fields to manipulate the valence manifolds of copper complexes. Chemical Science 2021, 12 (12), 4395–4404. [PubMed: 34163703]

(141). Crabtree RH Deactivation in Homogeneous Transition Metal Catalysis: Causes, Avoidance, and Cure. Chem. Rev. (Washington, DC, U. S.) 2015, 115 (1), 127–150.

(142). Clarke RM; Storr T Tuning Electronic Structure To Control Manganese Nitride Activation. J. Am. Chem. Soc 2016, 138 (47), 15299–15302. [PubMed: 27933934]

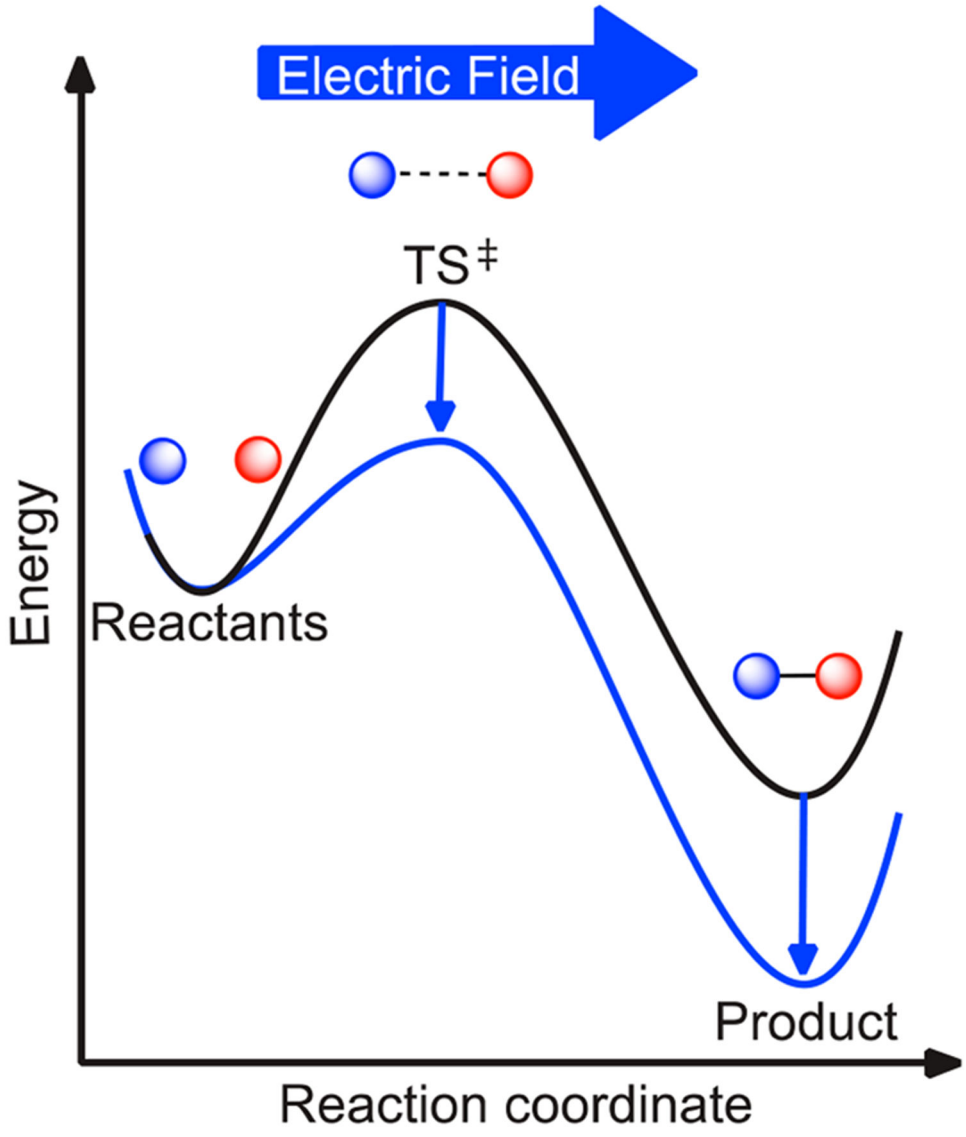

Figure 1.
Potential impact of electrostatics on reaction energetics.

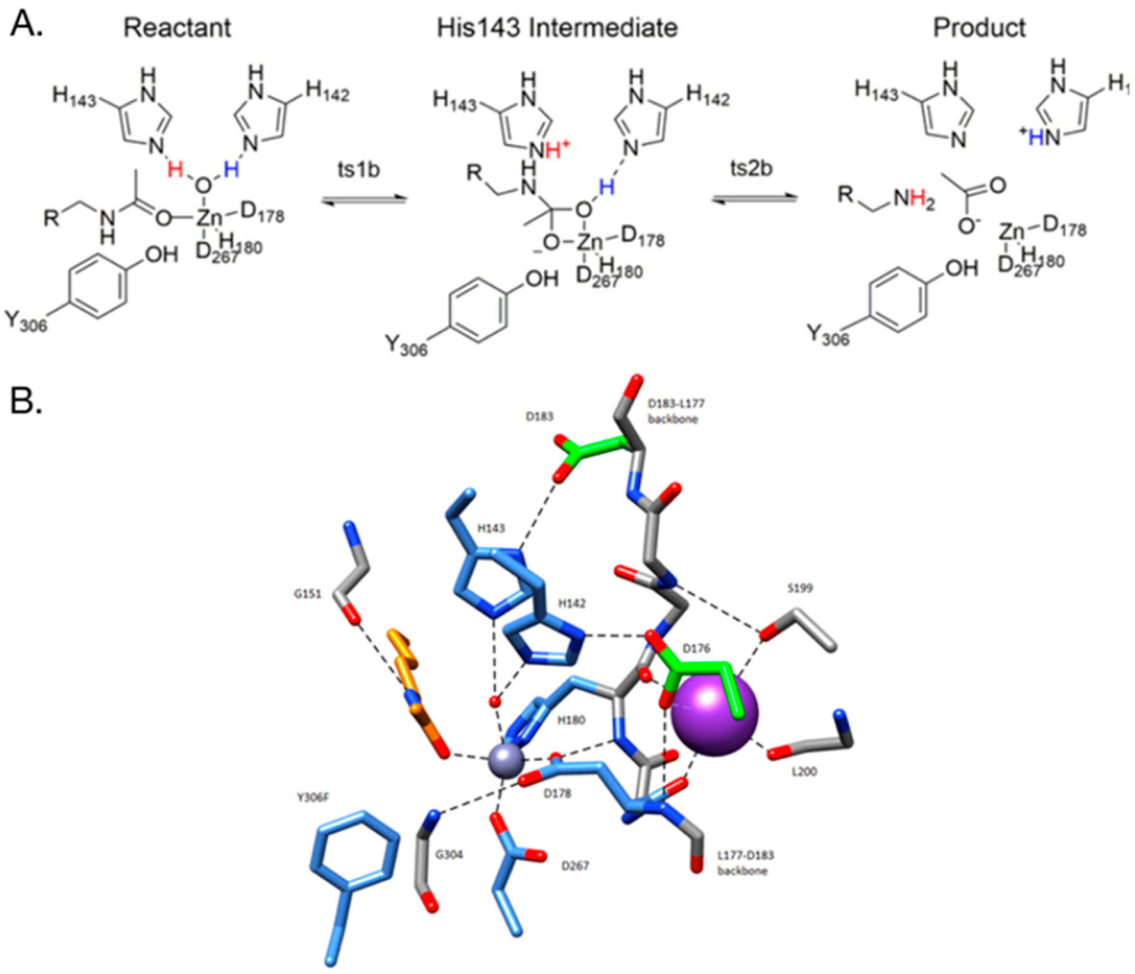

Figure 2.

A. Proton shuttle mechanism for HDAC8. B. Depiction of the active site of HDAC8 from a computational study. The system consists of the central Zn^{2+} ion (gray sphere), substrate (orange), K^{+} ion (purple sphere), and local residues. Reproduced with permission from ref 39. Copyright 2016 American Chemical Society.

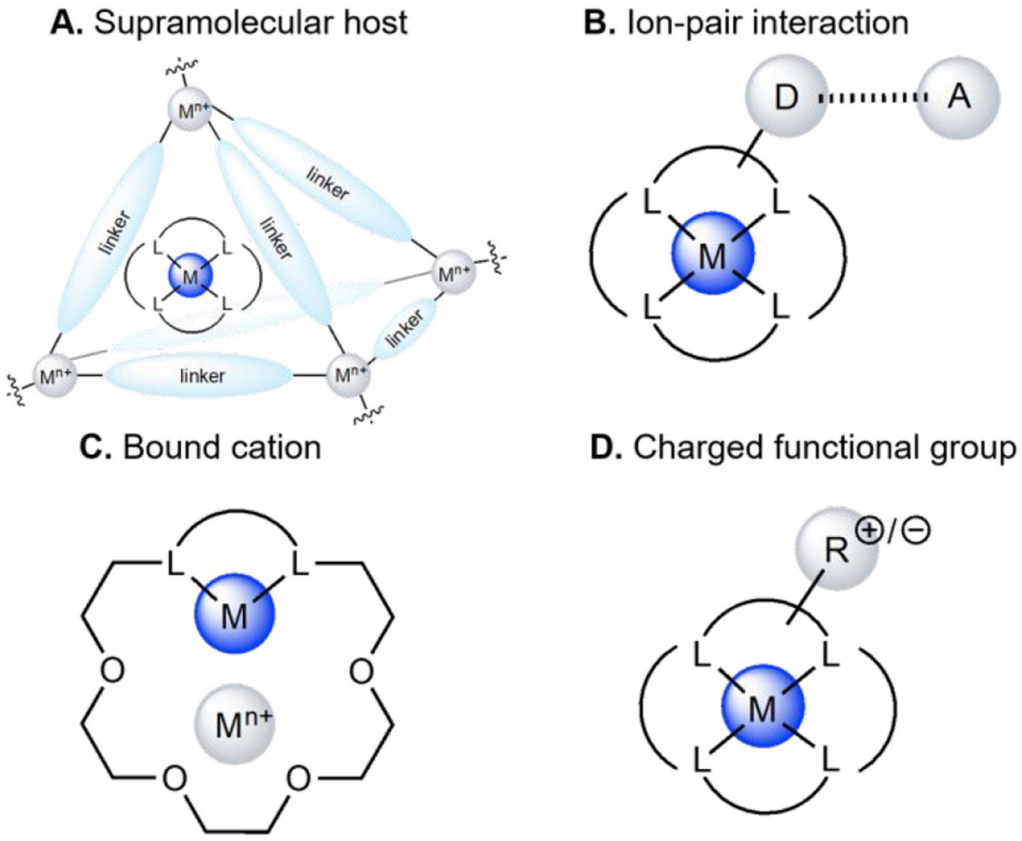

Figure 3.

Types of electrostatic interactions at transition metal complexes: A. Supramolecular host, B. Ion-pair interaction, C. Bound cation, D. Charged functional group. M = transition metal; L = ligand; D = ion-pair donor; A = ion-pair acceptor; $R^{\pm}$ = R'_3N^+, R'_3B^-, or M^{n+} = nonredox active metal.

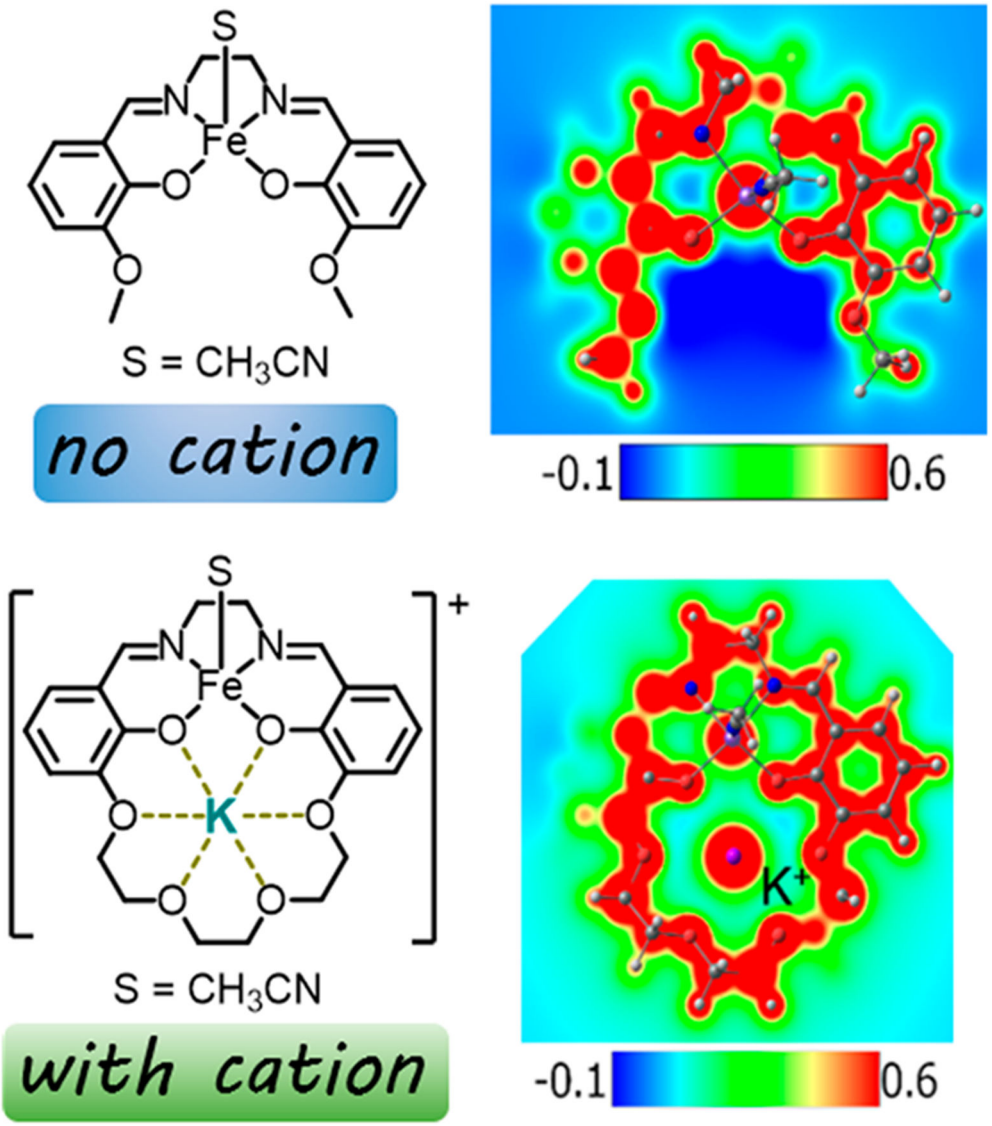

Figure 4.

Electrostatic potential maps of Fe(II) in a salen framework without (top) or with (bottom) a proximal K^+ cation. S = CH_3CN. Reproduced with permission from ref 123. Copyright 2019 The Royal Society of Chemistry.

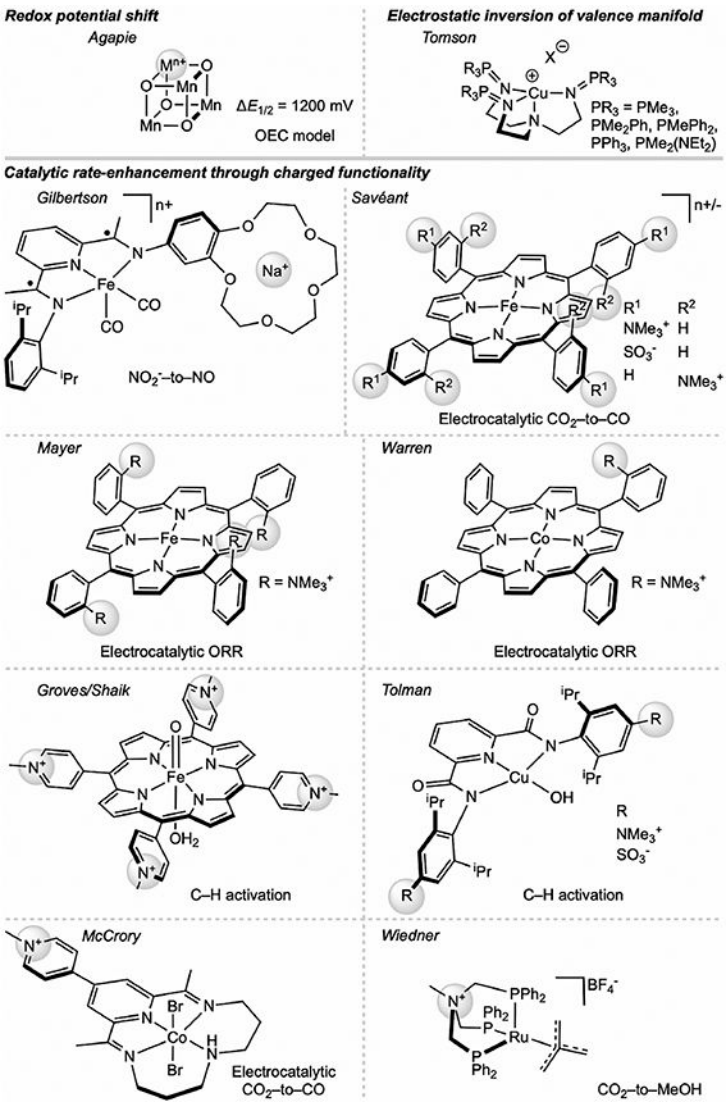

Figure 5.

Reported homogeneous transition metal complexes with charged functionalities that contribute to changes in electronic structure or reactivity. Left, top-to-bottom: Agapie (refs 125 and 126), Gilbertson (ref 127), Mayer (refs 130 and 131), Groves (refs 132 and 133), Shaik (ref 134), McCrory (ref 136); Right, top-to-bottom: Tomson (ref 140), Savéant (ref 128), Warren (ref 129), Tolman (ref 135), Wiedner (ref 137).